JOURNAL OF CHEMICAL EDUCATION

Article

pubs.acs.org/jchemeduc

Origin of the Anomalous Color of Egyptian and Han Blue Historical Pigments: Going beyond the Complex Approximation in Ligand Field Theory

Pablo García-Fernández, Miguel Moreno, and José Antonio Aramburu*

Departamento de Ciencias de la Tierra y Física de la Materia Condensada, Universidad de Cantabria, Avenida de los Castros s/n, 39005 Santander, Spain

Supporting Information

ABSTRACT: The complex approximation is widely used in the framework of the Ligand Field Theory for explaining the optical properties of crystalline coordination compounds. Here, we show that there are essential features of these systems that cannot be understood with the usual approximation that only considers an isolated complex at the correct equilibrium geometry. We also show that a quantitative understanding of such optical transitions cannot, in general, be reached unless the internal electric field, $\mathbf{E}_R(\mathbf{r})$, created by the whole crystal on active electrons confined in the complex, is also taken into consideration. Seeking to prove the key role played by this internal field, usually ignored in crystalline transition metal compounds, we focus on the origin of the color displayed by the Egyptian Blue pigment ($CaCuSi_4O_{10}$), the first ever synthesized by humans. This pigment, together with Han Blue ($BaCuSi_4O_{10}$), are chosen as model systems because the anisotropic $\mathbf{E}_R(\mathbf{r})$ field produces huge shifts, up to ∼0.9 eV, in their d−d transitions, which are unusual compared to the majority of compounds containing the same square-planar CuO_4^{6-} chromophore. The relevance of the internal field for explaining phenomena such as the distinct color of ruby and emerald or the optical spectrum of CuF_6^{4-} complexes in layered perovskites is also emphasized.

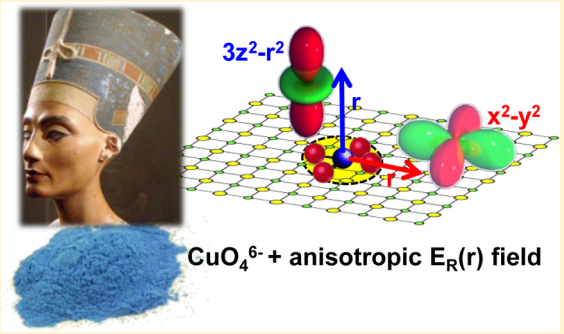

KEYWORDS: *General Public, First-Year Undergraduate/General, Theoretical Chemistry, UV-Vis Spectroscopy, Graduate Education/Research, Crystal Field/Ligand Field Theory, History/Philosophy, Inorganic Chemistry, Physical Chemistry, Misconceptions/Discrepant Events*

INTRODUCTION

The study of structural, optical and magnetic properties of coordination compounds is an important part of chemistry undergraduate programs.[1,2] According to the idea first put forward by Alfred Werner in 1893, the optical properties of an insulating crystal like $KNiF_3$ can essentially be understood only through the isolated NiF_6^{4-} complex, formed by the transition metal (TM) cation and the six nearest anions or ligands, where active electrons are actually confined.[3] More precisely, this statement means[4] that the optical properties of TM compounds are assumed to be determined only by (i) the nature of the TM cation and its ligands and also the coordination number; (ii) the geometrical arrangement of ligands; and (iii) the metal−ligand distances.

These ideas explain, for instance, why colors of $Co(NH_3)_4Cl_2$ complexes are different for *cis* and *trans* species as they involve a distinct arrangement of ligands and thus a distinct point symmetry. In the same vein, the optical transitions of a MnF_6^{4-} complex formed in $KMgF_3$:Mn^{2+} are shifted when the *same* unit is embedded in another isomorphous lattice like $KZnF_3$ or $CsCaF_3$.[4] This fact has been proved to reflect the variation experienced by the Mn^{2+}−F^- distance of the MnF_6^{4-} unit induced by the change of host lattice.[4]

In the early days of quantum mechanics, a first attempt to understand the properties of TM complexes was carried out through the rough crystal field model where ligands are simply treated as point charges.[3] Despite its crudeness, this model shows that the d-orbitals in an octahedral complex are no longer degenerate, but there is an energy difference, termed Δ_{oct} or 10 Dq,[2] between the pure σ and π d-orbitals usually designated, respectively, as $e_g(3z^2-r^2, x^2-y^2)$ and $t_{2g}(xy, xz, yz)$. Furthermore, according to this model, the octahedral crystal-field splitting, Δ_{oct}, is quite sensitive to changes of the metal−ligand distance, R, following the law[3]

$$\Delta_{oct} = KR^{-n} \quad (1)$$

where K is a specific constant for each metal−ligand bond and n = 5. Although experimental studies on octahedral complexes, like NiO_6^{10-}, MnF_6^{4-} or CrF_6^{3-}, embedded in host lattices are consistent with values of the exponent n not far from 5, the expression of Δ_{oct} derived in the crystal-field model usually fails

Published: November 6, 2015

DOI: 10.1021/acs.jchemed.5b00288
J. Chem. Educ. 2016, 93, 111−117

Figure 1. Egyptian Blue, Han Blue, and Han Purple pigments (adapted from ref 12 with permission from the Royal Society of Chemistry.

to reproduce the experimental values by 1 order of magnitude.[4] This big discrepancy stresses the existence of a covalent bonding between the TM cation and ligands which is thus fully disregarded in the coarse crystal-field description. In a further step, van Vleck pointed out that, to obtain a proper understanding of the properties related to coordination complexes, it is necessary to consider the suitable molecular orbitals involved in the complex, an idea that is the basis of the *traditional* ligand field theory (LFT).[3] Nevertheless, it is not until the arrival of the first quantum mechanical calculation performed on a TM complex that the experimental Δ_{oct} value is well reproduced.[5] Moreover, the seminal work by Sugano and Shulman on the isolated NiF_6^{4-} complex demonstrated that the Δ_{oct} splitting mainly arises from a different covalent bonding in $e_g(3z^2-r^2,\ x^2-y^2)$ and $t_{2g}(xy,\ xz,\ yz)$ molecular orbitals[5] involving a distinct hybridization of 3d nickel orbitals with 2p and 2s orbitals of fluorine. Subsequent theoretical work on other isolated octahedral complexes supported this conclusion finding at the same time that Δ_{oct} depends on R^{-n}, with n typically[4] in the range 3−6.

In accord with these results, the application of the *traditional* LFT in crystals has *assumed* that properties of coordination compounds can be explained just considering the isolated complex, where active electrons are localized, at the correct equilibrium distance. This standpoint is that essentially followed in significant textbooks.[3,6−9] Nevertheless, there are relevant experimental facts which cannot be understood through this truncated model such as it has been pointed out in recent years.[4,10] For instance, the different Δ_{oct} values of ruby (2.2 eV) and emerald (2.0 eV) have often been *assumed* to reflect a $Cr^{3+}-O^{2-}$ distance in the CrO_6^{9-} unit which is 0.06 Å smaller for $Al_2O_3:Cr^{3+}$ than for $Be_3Si_6Al_2O_{18}:Cr^{3+}$.[4,6−8] However, this assumption is against recent experimental and theoretical results showing that the Cr^{3+}-O^{2-} distance in both gemstones[10] is the same and equal to R = 1.97 Å. This fact already underlines that a *quantitative* understanding of optical data coming from TM compounds that only takes into account the isolated complex is, in general, not correct. At the same time, these results suggest the existence of another contribution to Δ_{oct} which is missing when we only consider the isolated CrO_6^{9-} complex for explaining the different color of ruby and emerald.

This puzzling situation is cleared up when one realizes that electrons localized in CrO_6^{9-} complexes are also subject to the electric field, $\mathbf{E}_R(\mathbf{r})$, generated by the rest of crystal ions, an internal field which is, in principle, different for Al_2O_3 and $Be_3Si_6Al_2O_{18}$ host lattices as they are not isomorphous.[4,10] The validity of this idea is supported by first-principles calculations. Indeed when the internal field, $\mathbf{E}_R(\mathbf{r})$, usually ignored in crystalline transition metal compounds, is included in the calculations they reproduce the 0.2 eV shift in Δ_{oct} observed when comparing ruby and emerald.[4,10]

It is worth noting now that Sugano and Shulman[5] in their pioneering work on TM compounds already analyzed the influence of the electric field, $\mathbf{E}_R(\mathbf{r})$, created by the rest of ions of the $KNiF_3$ perovskite on the electrons confined in NiF_6^{4-} units. Nevertheless, they concluded that, *for this simple perovskite lattice*, $\mathbf{E}_R(\mathbf{r})$ is negligible thus implying that optical properties of $KNiF_3$ can be explained just considering the isolated NiF_6^{4-} complex at its equilibrium distance. For this reason, it has usually been *assumed* that this situation can be extended for understanding the optical properties of other coordination compounds.[6−9] Nevertheless, the behavior of $\mathbf{E}_R(\mathbf{r})$ in the normal perovskite lattice has been shown to be an exception rather than a rule even if the host lattice is cubic.[4,10] For this reason, $\mathbf{E}_R(\mathbf{r})$, aside from explaining[10] the different color of ruby, emerald, alexandrite and Cr_2O_3, has been shown to be responsible for the distinct ground state of La_2CuO_4 and K_2CuF_4 compounds.[11]

The present work is addressed to demonstrate the key role played by the internal electric field, usually ignored in the realm of insulating TM compounds, pointing out that their properties cannot, in general, be properly understood through the idea of isolated complex. To achieve this goal, particular attention is paid to analyze the origin of the bright blue color of the first man-made pigment, known as Egyptian Blue.[12−15] This pigment is based on the $CaCuSi_4O_{10}$ crystal, and its optical properties are rather different from those of $CaCuO_2$, $BaCuSi_2O_6$ or Li_2CuO_2 compounds, all of them involving the *same* square-planar CuO_4^{6-} chromophore.[16] Aside from historical reasons, the Egyptian Blue pigment has been chosen as a *model system* for showing the shortcomings of considering only the isolated complex because the shifts induced by the internal field $\mathbf{E}_R(\mathbf{r})$ on the d−d transitions of the square−planar CuO_4^{6-} chromophore, up to ∼0.9 eV,[16] are much higher than those for other compounds involving octahedral complexes.[4,10]

DOI: 10.1021/acs.jchemed.5b00288
J. Chem. Educ. 2016, 93, 111−117

EGYPTIAN BLUE AND OTHER HISTORICAL PIGMENTS

It is well-known that in drawings found in prehistoric caves like Lascaux, Niaux or Altamira blue color is not present. In fact, while the rest of the palette could be obtained through iron and manganese oxides and coal, prehistoric men were not able to get stable minerals displaying a deep blue color.[12,13] This fact underlines the historical importance of the so-called Egyptian Blue pigment (Figure 1) already prepared around 3600 BC in the early Egyptian culture and widely employed not only in Egypt but also in Greece and the Roman Empire.[12−14] The fingerprint of this pigment is well found in Amarna, Luxor, or Pompeii with the crown of the famous bust of Queen Nefertiti being the best known example where pure Egyptian Blue was used.

Aside from being the first synthetically produced by mankind, the Egyptian Blue pigment is very stable and exhibits a bright blue color. This pigment contains a mixture of several phases such as cuprorivaite ($CaCuSi_4O_{10}$), unreacted quartz and variable amounts of glass[12−14] and its color comes from the square-planar CuO_4^{6-} chromophore involved in the $CaCuSi_4O_{10}$ compound,[15,16] which exhibits the gillespite, $BaFeSi_4O_{10}$, structure (tetragonal space group *P*4/*ncc*, see Figure 2). The

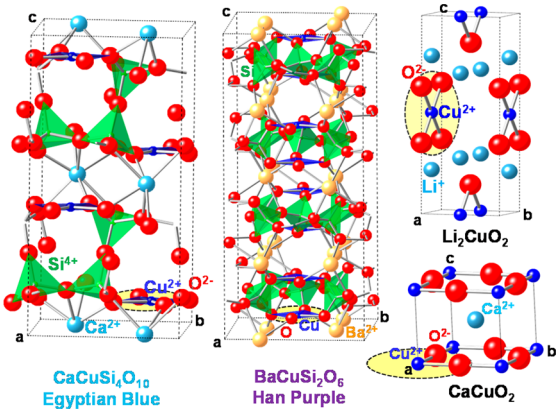

Figure 2. Unit cells corresponding to Egyptian Blue $CaCuSi_4O_{10}$ (and Han Blue $BaCuSi_4O_{10}$) pigment, Han Purple $BaCuSiO_2O_6$ pigment, $CaCuO_2$ and Li_2CuO_2 compounds. Cu^{2+} ions involved in square-planar CuO_4^{6-} complexes (yellow dotted circles) are depicted in dark blue, while SiO_4^{4-} tetrahedra are in green.

same structure and chromophore and a nearly identical color is displayed by $BaCuSi_4O_{10}$, which is the basis of the Han Blue pigment (Figure 1) developed during the Han dynasty (208 B.C.E. to 220 A.D.) in China,[12,16] together with the so-called Han Purple, identified, for example, in the terracotta warriors discovered in central China in 1974. The latter pigment contains $BaCuSi_2O_6$, which belongs to the $P4_1/acd$ space group (Figure 2). Although it also involves the CuO_4^{6-} chromophore, it does not exhibit a bright blue color like $ACuSi_4O_{10}$ (A = Ca, Ba).

At the fall of the Roman Empire, the knowledge of the Egyptian Blue technology disappeared almost abruptly, with the last written reference in the *Etymologiae* from Saint Isidore of Seville (7th century). However, recent works have found[17] that this pigment appears in some Byzantine frescos (9th century), a roman church in Spain (11th century), and some Cinquecento paints in Bologna (16th century).

During the Middle Age, the demand for blue pigments was met by lapis lazuli (also called ultramarine because it came from far Afghanistan via the port of Venice) or cobalt blue (also called Thenard's Blue or Dresden Blue), both very costly and thus reserved for the most important pictorial elements as, for example, Virgin robes. Aside from these pigments, blue was obtained principally from the much more abundant mineral azurite, $Cu_3(CO_3)_2(OH)_2$, which is, unfortunately, unstable in open air giving rise to malachite, $Cu_2(CO_3)(OH)_2$, which is green. For this reason, the use of the unstable azurite pigment for the delicate blue skies painted by Giotto in the "Scrovegni Chapel" frescoes in Padua (14th century) currently raises serious problems in the conservation of paintings and today the painted sky of the crucifixion in the "Santo Chiodo" chapel is visibly green.[18] This situation did not change until the 19th century when industrialization led to the chemical mass production of stable dyes and pigments.

The interest in the Egyptian Blue pigment reappeared with archeological excavations and subsequent chemical analysis of products. In particular, the discovery of a strong infrared luminescence of $CaCuSi_4O_{10}$[19,20] has been useful to detect its presence in old monuments like the Parthenon in Greece.

BLUE COLOR OF EGYTIAN BLUE AND HAN BLUE PIGMENTS IS UNEXPECTED

Although Egyptian Blue pigment plays an important role in human history, it is not easy to understand its color especially when compared with that of other compounds containing the *same* square-planar CuO_4^{6-} complex.[16] Indeed the blue color of $CaCuSi_4O_{10}$ or $BaCuSi_4O_{10}$ can be seen as *anomalous* in comparison with that displayed by $BaCuSi_2O_6$, Li_2CuO_2, or $CaCuO_2$ which have a simpler crystal structure (Figure 2). For specifying this key point experimental optical spectra in the visible region of $CaCuSi_4O_{10}$, and $BaCuSi_2O_6$ are compared in Figure 3, where data about *d*-*d* transitions in $CaCuO_2$ are also provided.[16]

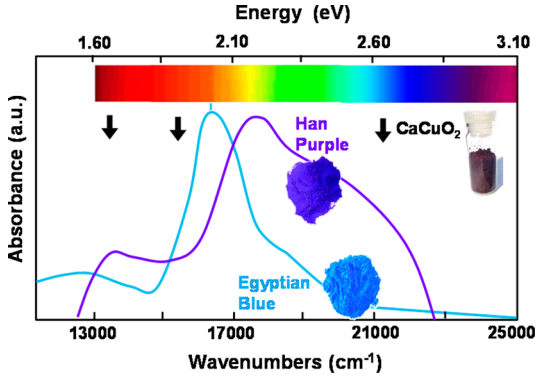

Figure 3. Experimental optical spectra in the visible region (intensities are not to scale) of Egyptian Blue ($CaCuSi_4O_{10}$) and Han Purple ($BaCuSi_2O_6$).[5] The d−d peak energies for $CaCuO_2$ are also shown as black arrows.[16]

As it is well-known, compounds containing square-planar CuO_4^{6-} complexes have three d−d transitions in the optical region (Figure 4) which give rise to three broad bands, such as it is shown in Figure 3. Table 1 shows experimental structural data and peak energies of three d−d bands corresponding to Egyptian Blue, Han Blue, and Han Purple pigments and $CaCuO_2$ and Li_2CuO_2 compounds, all of them involving

DOI: 10.1021/acs.jchemed.5b00288
J. Chem. Educ. 2016, 93, 111−117

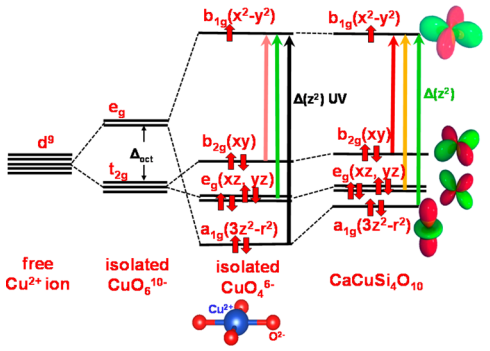

Figure 4. Qualitative diagram showing the splitting of d-levels of a Cu^{2+} ion in an octahedral CuO_6^{10-} complex, a square-planar CuO_4^{6-} complex, and a CuO_4^{6-} complex embedded in the $CaCuSiO_4O_{10}$ compound. Arrows represent the three d−d transitions and are colored according to the absorbed region of the spectrum. Note the great reduction of $\Delta(z^2)$ when passing from the isolated CuO_4^{6-} complex (energy in the ultraviolet, UV, region of the spectrum) to the same complex embedded in $CaCuSiO_4O_{10}$ (green region).

square-planar CuO_4^{6-} complexes.[15,16] We see that the peak energy of the band corresponding to the *highest* $a_{1g}(3z^2-r^2) \rightarrow b_{1g}(x^2-y^2)$ excitation, denoted $\Delta(z^2)$, is approximately 0.4 eV lower for Egyptian and Han Blue pigments than for the rest of compounds. This fact produces in Egyptian and Han Blue pigments the practical absence of absorption in the blue region (~2.45−2.65 eV) in striking contrast with the other systems. As the rest of the visible spectrum is absorbed by the three broad d−d transitions, this gives rise to the characteristic bright blue color exhibited by Egyptian and Han Blue pigments (Figures 1 and 3).

INCONSISTENCIES IN THE APPLICATION OF LFT FOR EXPLAINING THE COLOR OF EGYPTIAN BLUE AND HAN BLUE

As previously underlined, the optical spectra of TM cations in insulating compounds are usually analyzed considering only the isolated complex formed by the TM ion with the nearest anions or ligands. According to this view, the optical properties only depend on the chemical nature of the central cation and ligands, the point symmetry of the complex, and the metal−ligand distances between them.[3,6−9,15] However, these ideas are unable to explain the different energies observed for the d−d transitions of historical blue pigments when compared with those of $CaCuO_2$ or $BaCuSi_2O_6$ compounds, also involving square-planar CuO_4^{6-} complexes.[16]

In this sense, the effect of chemical substitution of ligands in octahedral complexes is usually *estimated* using the spectrochemical series.[1,2,16] Accordingly, taking the experimental value of the $a_{1g}(3z^2-r^2) \rightarrow b_{1g}(x^2-y^2)$ transition energy, $\Delta(z^2) = 2.11$ eV, for the square-planar $CuCl_4^{2-}$ chromophore in (*N*-mph)$_2$CuCl$_4$ (*N*-mph = *N*-methylphenethylammonium, [16] (C_6H_5)$CH_2CH_2NH_2(CH_3)^+$)), one would expect that when chlorine is replaced by oxygen as ligand, $\Delta(z^2)$ should be around 2.70 eV. This figure is however far from the experimental value for Egyptian Blue and Han Blue pigments but close to that measured for Han Purple, $CaCuO_2$ or Li_2CuO_2 as shown on Table 1. The 14% reduction in $\Delta(z^2)$ when comparing $CaCuO_2$ and $CaCuSi_4O_{10}$ could be explained, considering the *isolated* CuO_4^{6-} complex, *only if* the $Cu^{2+}-O^{2-}$ distance, *R*, is smaller for the former than for the latter compound as the splitting among d-levels is sensitive to variations of *R*. However, X-ray diffraction measurements give $R = 1.928$ Å for the Cu^{2+}-O^{2-} distance in $CaCuSi_4O_{10}$, a value practically equal to $R = 1.929$ Å corresponding to $CaCuO_2$ (Table 1). Furthermore, as the $Cu^{2+}-O^{2-}$ distance in Egyptian Blue is smaller than that measured for Li_2CuO_2 ($R = 1.959$ Å) or $BaCuSi_2O_6$ ($R = 1.945$ Å), it could be expected that $\Delta(z^2)$ should be higher for the former than for the latter compounds if we only consider the *isolated* CuO_4^{6-} complex. As these predictions are *all in contradiction* with experimental findings, this proves that no reasonable explanation of them can be reached within the *traditional* LFT, devoted to explain the experimental optical data on the basis of isolated complexes.

INTERNAL ELECTRIC FIELD ON THE CuO_4^{6-} COMPLEX FROM THE REST OF LATTICE IONS

The key role played by the internal field, $\mathbf{E}_R(\mathbf{r})$, for understanding the anomalous behavior of d−d transitions in Egyptian and Han Blue pigments is analyzed in this section. With the objective of clearing up this issue, the results obtained by means of density functional theory (DFT) calculations (see Supporting Information file and ref 16 for computational details) are given in Table 2. Aside from the values of d−d transitions derived for an *isolated* CuO_4^{6-} complex at $R = 1.928$ Å (Table 2), those obtained including the influence of the $V_R(\mathbf{r})$ potential, generating the internal field, $\mathbf{E}_R(\mathbf{r})$, through $\mathbf{E}_R(\mathbf{r}) = -\nabla V_R(\mathbf{r})$, are also reported. Moreover, the d−d

Table 2. Calculated Energies (eV) of the d−d Transitions for Egyptian Blue ($CaCuSi_4O_{10}$) and $CaCuO_2$

	CuO_4^{6-} and $V_R(\mathbf{r})$[a]		
Transitions	$CaCuSi_4O_{10}$[c]	$CaCuO_2$[c]	Isolated CuO_4^{6-}[b]
$b_{2g}(xy) \rightarrow b_{1g}(x^2-y^2)$	1.49 [1.58]	1.54 [1.64]	~1.75
$e_g(xz,yz) \rightarrow b_{1g}(x^2-y^2)$	1.98 [2.00]	1.93 [1.95]	~2.33
$a_{1g}(3z^2-r^2) \rightarrow b_{1g}(x^2-y^2)$	2.43 [2.30]	2.75 [2.65]	~3.31

[a]Adding the electrostatic potential $V_R(\mathbf{r})$ of $CaCuSi_4O_{10}$ and $CaCuO_2$ lattices. [b]Extrapolation to the zero-field limit for the CuO_4^{6-} complex at $R = 1.928$ Å using the data in Figure 5. [c]Experimental values[16] are given in square brackets.

Table 1. Experimental Values of the Cu^{2+}-O^{2-} Distances, *R* (in Å), and Peak Energies (in eV) of the Three d−d Transitions for Some Compounds Containing CuO_4^{6-} Complexes[16]

	$CaCuSi_4O_{10}$ Egyptian Blue	$BaCuSi_4O_{10}$ Han Blue	$BaCuSi_2O_6$ Han Purple	$CaCuO_2$	Li_2CuO_2
Space Group	*P4/ncc*	*P4/ncc*	$P4_1/acd$	*P4/mmm*	*Immm*
R	1.928	1.921	1.945	1.929	1.959
$b_{2g}(xy) \rightarrow b_{1g}(x^2-y^2)$	1.58	1.60	1.67	1.64	1.74
$e_g(xz,yz) \rightarrow b_{1g}(x^2-y^2)$	2.00	1.96	2.11	1.95	2.11
$a_{1g}(3z^2-r^2) \rightarrow b_{1g}(x^2-y^2)$	2.30	2.33	~ 2.60	2.65	~ 2.72

DOI: 10.1021/acs.jchemed.5b00288
J. Chem. Educ. 2016, 93, 111−117

Table 3. Experimental Energies, Δ(exper), of Selected Optical Transitions of Several Compounds Containing TM Complexes and Values of the Corresponding Extrinsic Contribution, Δ_{ext}, Derived from Calculations[16]

System	Complex	Optical Transition	Δ(exper) (eV)	Δ_{ext} (eV)
Ruby	CrO_6^{9-}	$^4A_2(t_{2g}^3) \rightarrow {}^4T_2(t_{2g}^2e_g^1)^a$	2.24	+0.24
Emerald	CrO_6^{9-}	$^4A_2(t_{2g}^3) \rightarrow {}^4T_2(t_{2g}^2e_g^1)^a$	2.0	−0.05
MgO:Cr^{3+}	CrO_6^{9-}	$^4A_2(t_{2g}^3) \rightarrow {}^4T_2(t_{2g}^2e_g^1)^a$	2.0	+0.21
K_2ZnF_4:Cu^{2+}	CuF_6^{4-b}	$a_{1g}(3z^2-r^2) \rightarrow b_{1g}(x^2-y^2)$	∼ 0.70	+0.34
$CaCuSi_4O_{10}$	CuO_4^{6-}	$a_{1g}(3z^2-r^2) \rightarrow b_{1g}(x^2-y^2)$	2.30	−0.88
$CaCuO_2$	CuO_4^{6-}	$a_{1g}(3z^2-r^2) \rightarrow b_{1g}(x^2-y^2)$	2.65	−0.56

[a]The value of the first allowed transition, $^4A_2(t_{2g}^3) \rightarrow {}^4T_2(t_{2g}^2e_g^1)$ for octahedral Cr^{3+} complexes is just equal[9] to the Δ_{oct} value. [b]In K_2ZnF_4:Cu^{2+} the CuF_6^{4-} unit has a slight tetragonal distortion that only explains ∼50% of the experimental $a_{1g}(3z^2\text{-}r^2) \rightarrow b_{1g}(x^2\text{-}y^2)$ transition energy.[21]

transitions calculated for a CuO_4^{6-} unit under the internal potential, $V_R(\mathbf{r})$, due to $CaCuSi_4O_{10}$ and $CaCuO_2$, are given in Table 2 as well.

It can be seen in Table 2 and Figure 4 that the d−d transition with the highest energy is always the $a_{1g}(3z^2-r^2) \rightarrow b_{1g}(x^2-y^2)$ one, a situation quite different to that encountered in a distorted octahedral unit, due the lack of axial ligands in a true square−planar complex. Furthermore, it is worth noting in Table 2 that only when $\mathbf{E}_R(\mathbf{r})$ is incorporated into the calculation are the d−d transitions observed in $CaCuSi_4O_{10}$ and $CaCuO_2$ reasonably reproduced by the calculations. Indeed, it is shown that $\mathbf{E}_R(\mathbf{r})$ in $CaCuSi_4O_{10}$ induces a strong reduction of 0.88 eV on the $a_{1g}(3z^2-r^2) \rightarrow b_{1g}(x^2-y^2)$ transition energy when compared to the value $\Delta(z^2)$ = 3.31 eV derived for the isolated CuO_4^{6-} unit at R = 1.928 Å. This big reduction due to $\mathbf{E}_R(\mathbf{r})$ is thus responsible for placing the $a_{1g}(3z^2-r^2) \rightarrow b_{1g}(x^2-y^2)$ transition of $CaCuSi_4O_{10}$ at an energy below the blue region (∼2.45−2.65 eV), thus stressing the key role played by the internal field for understanding the color of the Egyptian Blue pigment. In the case of $CaCuO_2$, the results conveyed in Table 2 show that the internal field, $\mathbf{E}_R(\mathbf{r})$, also leads to a decrease of 0.56 eV in the $\Delta(z^2)$ value. This reduction, which is significantly smaller than that found for $CaCuSi_4O_{10}$, thus explains why the experimental value of $\Delta(z^2)$ for this compound is about 0.40 eV smaller than that for $CaCuO_2$.

The present analysis thus proves that for a complex embedded in a crystal lattice there are actually two contributions[10] to a given transition energy, Δ,

$$\Delta = \Delta_{int} + \Delta_{ext} \quad (2)$$

The first one, Δ_{int}, is the intrinsic contribution, which already appears taking the *isolated* complex at the right equilibrium geometry. For octahedral complexes the transition energy, Δ, associated with d−d transitions often depends on Δ_{oct}. In the case of an *isolated* complex Δ_{oct} is found[4] to be quite sensitive to changes of the metal−ligand distance, R, whose actual microscopic origin is discussed in ref 4. The second term in eq 2, Δ_{ext}, is the *extrinsic* contribution to the complex, directly induced by the internal field, $\mathbf{E}_R(\mathbf{r})$, which has usually been ignored in the study of insulating TM compounds.[4,10]

For the sake of clarity, in addition to data corresponding to $CaCuSi_4O_{10}$ and $CaCuO_2$, representative values of the extrinsic contribution for some d−d transitions of TM complexes are collected in Table 3. It can be noticed that although Δ_{ext} is always smaller than the transition energy, Δ, it allows one to understand why ruby and emerald exhibit a different color despite R = 1.97 Å is the same for both gemstones, or why MgO:Cr^{3+}, where R = 2.03 Å, has the same Δ_{oct} value as in emerald.[10] Also the data in Table 1 emphasize that ∼50% of the splitting between $3z^2-r^2$ and x^2-y^2 orbitals in K_2ZnF_4:Cu^{2+} is due to the action of the internal field and not to the slight tetragonal distortion in the CuF_6^{4-} complex.[21] Interestingly, the results conveyed in Table 3 show that the highest values of $|\Delta_{ext}|$ are reached for the $a_{1g}(3z^2-r^2) \rightarrow b_{1g}(x^2-y^2)$ transition of $CaCuO_2$ and, especially, $CaCuSi_4O_{10}$. Why the extrinsic contribution for these systems is negative and why $|\Delta_{ext}|$ is higher for $CaCuSi_4O_{10}$ than $CaCuO_2$ is discussed later in some detail.

It is worth noting now that an isolated CuO_4^{6-} complex is unstable as it is highly charged. Therefore, for properly calculating the d−d transition energies for an isolated complex given in Table 2, first-principles calculations have been performed[16] using a rescaled potential $\lambda V_R(\mathbf{r})$ with $0 \le \lambda \le 1$ for both $CaCuSi_4O_{10}$ and $CaCuO_2$ compounds. It has been found that calculations can be carried out in the $0.5 \le \lambda \le 1$ range for both lattices, but when $\lambda \le 0.4$, the self-consistent field (SCF) convergence cannot be achieved. Despite this fact, if we extrapolate the results obtained for a given d−d transition of the CuO_4^{6-} complex in the $0.5 \le \lambda \le 1$ range to the zero-field limit (λ = 0, see Figure 5), we find the *same* value for

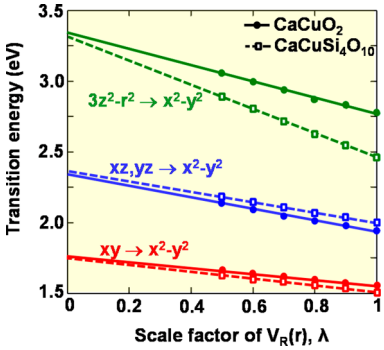

Figure 5. Variation of the three d−d transition energies for a square-planar CuO_4^{6-} complex subject to a scaled embedding potential $\lambda V_R(\mathbf{r})$. Full circle and empty square markers correspond to calculated energies in the $0.5 \le \lambda \le 1$ range for $CaCuO_2$ and $CaCuSi_4O_{10}$, respectively.

$CaCuSi_4O_{10}$ and $CaCuO_2$ compounds. Therefore, this important result implies that transitions obtained in the zero-field limit can be considered to be those corresponding to the *in vacuo* complex even if this isolated species is unstable.

Moreover, the fact that the variation of the transition with the scaling factor is linear shows that no significant changes in the copper−oxygen covalency or the 3d−4s hybridization in Cu are taking place (which would show up as a parabolic contribution in Figure 5) with the introduction of $\mathbf{E}_R(\mathbf{r})$. Thus, the correct understanding of the change in the transitions with respect to an *in vacuo* example simply corresponds with

DOI: 10.1021/acs.jchemed.5b00288
J. Chem. Educ. 2016, 93, 111−117

the effect of a field on a *fixed* electron density (first-order contributions in a quantum mechanical treatment).[10]

Meaning of the Internal Electric Field, $E_R(r)$

Let us consider a MX_N complex placed in a crystalline lattice, R being the metal−ligand distance. If the M cation is placed at the origin, it is well-known that *all ions* lying outside a given complex contribute to $V_R(\mathbf{0})$. In fact this quantity is simply related[10] to the *long-range* Madelung potential felt by the M cation, $V_M(\mathbf{0})$, by

$$V_M(\mathbf{0}) = V_R(\mathbf{0}) + NQ_X/R \quad (3)$$

where Q_X stands for the charge of a ligand. Nevertheless, not all ions of the rest of the lattice actually contribute to the internal field on the complex, $\mathbf{E}_R(\mathbf{r})$. This issue can be cleared up through two significant considerations. First, if we designate by $\rho_R^+(\mathbf{r})$ and $\rho_R^-(\mathbf{r})$ the charge density associated with positive and negative charges of the rest of the lattice, the internal field created on the complex is null if both $\rho_R^+(\mathbf{r})$ and $\rho_R^-(\mathbf{r})$ display spherical symmetry. This is a simple consequence of the Gauss theorem and thus of the Coulomb law in electrostatics, implying that under such conditions $V_R(\mathbf{r})$ is constant through the complex region. On the other hand, a charge q lying at a distance R_q from the central cation essentially produces a constant potential on the whole complex region, equal to q/R_q, provided $R_q \gg R$. According to these reflections, $\mathbf{E}_R(\mathbf{r})$, which actually depends on $[V_R(\mathbf{r}) - V_R(\mathbf{0})]$, arises from the departures from spherical symmetry of shells of ions lying close to the complex. Aside from proving the validity of this idea for ruby and emerald,[10] it has been shown that the near absence of internal field in the perovskite lattice can be explained just considering the first two shells lying outside the complex.[4,10]

Internal Electrostatic Potential for Different Compounds Containing the CuO_4^{6-} Complex

From the analysis carried out in previous sections an electron of charge $-e$ confined in the CuO_4^{6-} complex is also subject to the potential energy $(-e)[V_R(\mathbf{r}) - V_R(0)]$ associated with the internal field $\mathbf{E}_R(\mathbf{r})$. A qualitative understanding of the effect of $(-e)[V_R(\mathbf{r}) - V_R(0)]$ over the $a_{1g}(3z^2-r^2) \rightarrow b_{1g}(x^2-y^2)$ transition in $CaCuSi_4O_{10}$ and $CaCuO_2$ crystals is simply reached noting that the orbitals involved in this electron excitation are directed in orthogonal directions. So, while the $a_{1g}(3z^2-r^2)$ orbital is mainly localized along an axis perpendicular to the CuO_4^{6-} complex plane, the $b_{1g}(x^2-y^2)$ orbital has a planar character with its maximum density along the Cu−O bond directions (Figure 6).

Comparing the shape of $[V_R(\mathbf{r}) - V_R(0)]$ along these directions (Figure 6) for both $CaCuSi_4O_{10}$ and in $CaCuO_2$, we see that they are qualitatively similar. Taking as reference the isolated CuO_4^{6-} complex, the addition of the internal field, $\mathbf{E}_R(\mathbf{r})$, leads to an energy reduction for the higher x^2-y^2 orbital and especially an energy increase for the $3z^2-r^2$ orbital. These changes induced by $\mathbf{E}_R(\mathbf{r})$ imply a decrease of the $a_{1g}(3z^2-r^2) \rightarrow b_{1g}(x^2-y^2)$ transition energy and thus a negative extrinsic contribution. However, it can be seen in Figure 6 that the intensity of $[V_R(\mathbf{r}) - V_R(0)]$ is stronger in Egyptian Blue than in $CaCuO_2$. This fact leads to a higher value of $|\Delta_{ext}|$ and a more substantial reduction of $\Delta(z^2)$ for $CaCuSi_4O_{10}$ which is thus responsible for the energy shift that prevents the absorption of blue light in this compound. In a further analysis, it has been shown[16] that the shape of $(-e)[V_R(\mathbf{r}) - V_R(0)]$ in $CaCuSi_4O_{10}$ (Figure 6) is mainly due to SiO_4^{4-} units.

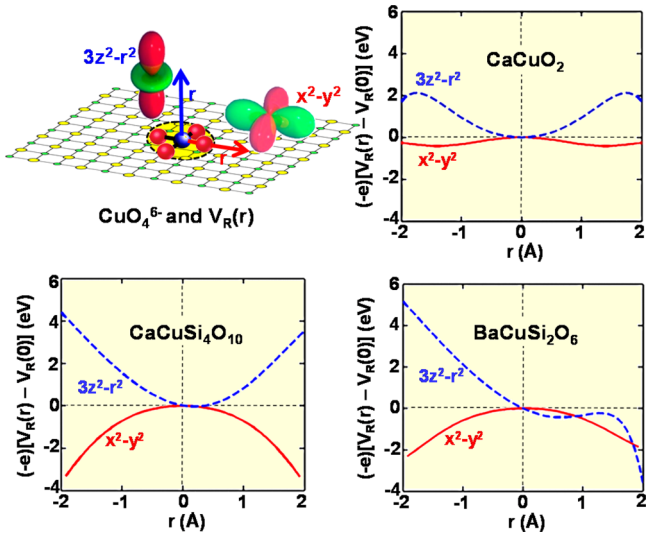

Figure 6. Shape of the variation of $(-e)[V_R(\mathbf{r}) - V_R(0)]$ potential energy felt by an electron of the CuO_4^{6-} complex when the electron coordinate $\mathbf{r}$ moves either along the in-plane Cu−O bond (solid red lines) or the axial OZ (dashed blue lines) directions mainly perturbing, respectively, the $b_{1g}(x^2 - y^2)$ and $a_{1g}(3z^2 - r^2)$ orbitals. Results for $CaCuSi_4O_{10}$, $BaCuSi_2O_6$ and $CaCuO_2$ crystals are reported.[16]

Therefore, although such units are not involved in the chromophore itself, the introduction of *sand* to create $CaCuSi_4O_{10}$ plays a key role to modify the $(-e)[V_R(\mathbf{r}) - V_R(0)]$ potential thus helping the compound to display its characteristic blue color.

A Complex in Different Isomorphous Lattices: Comparison between Egyptian Blue and Han Blue

As previously shown, the differences in the d−d transition energies of $CaCuSi_4O_{10}$, $CaCuO_2$ and $BaCuSi_2O_6$ are greatly due to the distinct extrinsic contribution, Δ_{ext}, in the three compounds which reflects the different shape displayed by the internal $[V_R(\mathbf{r}) - V_R(\mathbf{0})]$ quantity in the three non isomorphous lattices. Contrastingly, when the same complex is placed in a series of true isomorphous lattices, the variations undergone by optical transitions essentially arise from the change undergone by the dominant intrinsic contribution, which in turn reflects the change of the metal−ligand distance, R, along the series.[4,10] According to this view the change of the octahedral-field splitting parameter, Δ_{oct}, along the series of cubic fluoroperovskites like $KMgF_3$ or $CaCaF_3$ doped with Mn^{2+} or Ni^{2+} impurities or cubic elpasolites containing Cr^{3+} cations essentially reflects the change of the impurity-ligand distance, R, imposed by the host lattice.[4] Therefore, in the referred cases, involving series of isomorphous lattices, the changes in optical properties can be well accounted for only through isolated MF_6^{4-} (M = Mn, Ni) or CrF_6^{3-} complexes at the correct equilibrium distance.

That situation is also encountered when comparing Egyptian Blue ($CaCuSi_4O_{10}$) and Han Blue ($BaCuSi_4O_{10}$) pigments as both compounds have isomorphous structures and, therefore, the internal potential in both lattices is essentially coincident. The slightly different tonality of both pigments can merely be explained by the small 0.36% reduction in Cu−O distance when going from $BaCuSi_4O_{10}$ (R = 1.921 Å) to $CaCuSi_4O_{10}$ (R = 1.929 Å). Indeed, the calculations[16] predict an increase of 0.045 eV in $\Delta(z^2)$ when changing the Cu−O distance from

DOI: 10.1021/acs.jchemed.5b00288
J. Chem. Educ. 2016, 93, 111−117

1.929 to 1.921 Å, which is not far from the experimental variation of 0.035 eV (Table 1).

CONCLUSIONS

As a main conclusion, the present work proves that the optical properties of insulating TM compounds cannot, in general, be understood considering only the isolated complex. Indeed, they also depend on the internal electric field, $\mathbf{E}_R(\mathbf{r})$, created by the rest of lattice ions on the complex where active electrons reside, a fact usually ignored in the realm of inorganic TM compounds. As a relevant example, it has been shown that such an internal field plays a key role for understanding the bright blue color displayed by the Egyptian Blue pigment ($CaCuSi_4O_{10}$), the first synthetically produced pigment in human history. In fact, $\mathbf{E}_R(\mathbf{r})$ in $CaCuSi_4O_{10}$ induces a strong red shift (~0.9 eV) of the highest energy d−d transition with respect to what is found for an isolated CuO_4^{6-} complex. At the same time, the different shape of $\mathbf{E}_R(\mathbf{r})$ in $CaCuSi_4O_{10}$ and $CaCuO_2$ reasonably explains the distinct d−d transitions observed experimentally in such compounds involving the same CuO_4^{6-} complex and the same Cu^{2+}-O^{2-} distance. In the same vein, the different internal electric field in ruby and emerald is responsible for the disparate color displayed by these gemstones. Nevertheless, the extrinsic contribution[4,10] to Δ_{oct} in ruby, where Cr^{3+} is 6-fold coordinated, is only of ~0.2 eV and thus clearly smaller than that found in $CaCuSi_4O_{10}$ involving a square−planar CuO_4^{6-} complex.

We would like to finish noting that the biochemistry community[22,23] appears to pay more attention to the role of internal fields than inorganic or solid-state chemists. In fact, several recent papers deal with the importance of the electrostatic field over chromophores, like those created by amino acids in the opsin protein over the retinal chromophore,[22] a key feature to understand human vision, or the mechanism for light emission in the firefly luminiscent protein.[23]

ASSOCIATED CONTENT

Supporting Information

The Supporting Information is available on the ACS Publications website at DOI: 10.1021/acs.jchemed.5b00288.

Computational details (PDF, DOCX)

AUTHOR INFORMATION

Corresponding Author

* E-mail: aramburj@unican.es.

Notes

The authors declare no competing financial interest.

ACKNOWLEDGMENTS

This work was supported by the Spanish Ministerio de Economía y Competitividad under Projects FIS2012-30996 and FIS2012-37549-C05-4. P. Garcia-Fernandez acknowledges a fellowship from the Ramon y Cajal program. We acknowledge Keith Schengili-Roberts for giving us permission to use in the graphical abstract his personal photography of the Nefertiti bust exhibit in the Neus Museum of Berlin.

REFERENCES

(1) Brown, T. L.; LeMay, Jr., H. E.; Bursten, B. E., Murphy, C. J.; Woodward, P. M. *Chemistry: The Central Science*; Prentice Hall: Boston, 2012.
(2) Housecroft, C. E.; Sharpe, A. G. *Inorganic Chemistry*; Prentice Hall: Boston, 2012.
(3) Ballhausen, C. J. *Introduction to Ligand Field Theory*; McGraw-Hill: New York, 1962.
(4) Moreno, M.; Barriuso, M. T.; Aramburu, J. A.; Garcia-Fernandez, P.; Garcia-Lastra, J. M. Microscopic Insight into Properties and Electronic Instabilities of Impurities in Cubic and Lower Symmetry Insulators: The Influence of Pressure. *J. Phys.: Condens. Matter* **2006**, *18*, R315−R360.
(5) Sugano, S.; Shulman, R. G. Covalency Effects in KNiFs. III. Theoretical Studies. *Phys. Rev.* **1963**, *130*, 517−530.
(6) Nassau, K. *The Physics and Chemistry of Color*; Wiley: New York, 1983.
(7) Burns, R. G. *Mineralogical Applications of Crystal-Field Theory*; Cambridge UP: New York, 1993.
(8) Tilley, R. *Colour and the Optical Properties of Materials*; Willey: New York, 2011.
(9) Sugano, S.; Tanabe, Y.; Kamimura, H. *Multiplets of Transition-Metal Ions in Crystals*; Academic Press: New York, 1970.
(10) Aramburu, J. A.; Garcia-Fernandez, P.; Garcia-Lastra, J. M.; Barriuso, M. T.; Moreno, M. Colour Due to Cr^{3+} Ions in Oxides: A Study of the Model System MgO:Cr^{3+}. *J. Phys.: Condens. Matter* **2013**, *25*, 175501−17558 and further references therein..
(11) García-Fernández, P.; Moreno, M.; Aramburu, J. A. Electrostatic Control of Orbital Ordering in Noncubic Crystals. *J. Phys. Chem. C* **2014**, *118*, 7554−7561.
(12) Berke, H. The Invention of Blue and Purple Pigments in Ancient Times. *Chem. Soc. Rev.* **2007**, *36*, 15−30.
(13) Orna, M. Chemistry, Color, and Art. *J. Chem. Educ.* **2001**, *78*, 1305−1309.
(14) Loyson, P. Chemistry in the Time of the Pharaohs. *J. Chem. Educ.* **2011**, *88*, 146−150.
(15) Ford, R. J.; Hitchman, M. A. Single Crystal Electronic and EPR Spectra of $CaCuSi_4O_{10}$, a Synthetic Silicate Containing Copper in a Four-Coordinate, Planar Ligand Environment. *Inorg. Chim. Acta* **1979**, *33*, L167−L170.
(16) García-Fernández, P.; Moreno, M.; Aramburu, J. A. Origin of the Exotic Blue Colour of Copper-Containing Historical Pigments. *Inorg. Chem.* **2015**, *54*, 192−199 and further references therein..
(17) McCouat, P. *J. Art. Soc.* **2014**; http://www.artinsociety.com/egyptian-blue-the-colour-of-technology.html (accessed Aug 2015).
(18) Milanesi, C.; Baldib, F.; Borinc, S.; Vignania, R.; Ciampolinic, F.; Faleria, C.; Cresti, M. Biodeterioration of a Fresco by Biofilm Forming Bacteria. *Int. Biodeterior. Biodegrad.* **2006**, *57*, 168−173.
(19) Accorsi, G.; Verri, G.; Bolognesi, M.; Armaroli, N.; Clementi, C.; Miliani, C.; Romani, A. The Exceptional Near-Infrared Luminescence Properties of Cuprorivaite (Egyptian Blue). *Chem. Commun.* **2009**, 3392−3394.
(20) Johnson-McDaniel, D.; Barrett, C. A.; Sharafi, A.; Salguero, T. T. Nanoscience of an Ancient Pigment. *J. Am. Chem. Soc.* **2013**, *135*, 1677−1679.
(21) Garcia-Fernandez, P.; Barriuso, M. T.; Garcia-Lastra, J. M.; Moreno, M.; Aramburu, J. A. Compounds Containing Tetragonal Cu^{2+} Complexes: Is the $d_{x^2-y^2}$-$d_{3z^2-r^2}$ Gap a Direct Reflection of the Distortion? *J. Phys. Chem. Lett.* **2013**, *4*, 2385−2390.
(22) Fujimoto, K.; Hasegawa, J.; Nakatsuji, H. Origin of Color Tuning in Human Red, Green, and Blue Cone Pigments: SAC-CI and QM/MM Study. *Chem. Phys. Lett.* **2008**, *462*, 318−320.
(23) Cai, D.; Marques, M. A. L.; Nogueira, F. Full Color Modulation of Firefly Luciferase through Engineering with Unified Stark Effect. *J. Phys. Chem. B* **2013**, *117*, 13725−13730.

DOI: 10.1021/acs.jchemed.5b00288
J. Chem. Educ. 2016, 93, 111−117